A study on effects of size and structure on hygroscopicity of nanoparticles using a tandem differential mobility analyzer and TEM

Kihong Park · Jae-Seok Kim · Arthur L. Miller

Abstract A hygroscopicity tandem differential mobility analyzer (HTDMA) technique is used to determine size-effect of nanoparticles (NaCl, $(NH_4)_2SO_4$, KCl, NH_4NO_3, $MgCl_2$, $CaCl_2$) on their hygroscopic properties (deliquescence relative humidity (DRH) and hygroscopic growth factor (GF)). The HTDMA system uses a combination of two nano DMAs and two regular DMAs to measure particle size change in a wide dynamic particle size range. Particles are subsequently analyzed with a transmission electron microscopy to investigate the potential effect of particle structure or morphology on the hygroscopic properties. We found that structural properties of NaCl and $(NH_4)_2SO_4$ particles also play an important role in determination of the DRH and GF and are more pronounced at smaller diameters. Data show that the DRH of NaCl nanoparticles increased from $\sim 75\%$ up to $\sim 83\%$ RH at 8 nm and that their GF decreased with decreasing size. The extent to which the GF of NaCl nanoparticles decreased with decreasing size was greater than theoretically predicted with the Kelvin correction. The GF of furnace-generated NaCl nanoparticles that have pores and aggregate shape was found to be smaller than that of atomizer-generated particles that are close to perfectly cubic. For the case of atomizer-generated $(NH_4)_2SO_4$ nanoparticles, we observed no significant size-effect on their DRH, and the measured GF agreed well with predicted values using the Kelvin correction. For furnace-generated $(NH_4)_2SO_4$ nanoparticles, a gradual growth at moderate RH without noticeable deliquescence behavior occurred. Their TEM images showed that contrary to atomizer-generated $(NH_4)_2SO_4$ nanoparticles the furnace-generated $(NH_4)_2SO_4$ nanoparticles are not perfectly spherical and are often aggregates having pores and holes, which may favor holding residual water even in the dried condition. For atomizer-generated KCl, $MgCl_2$, and $CaCl_2$ nanoparticles, we observed no significant size-effects on their DRH and GF for the mobility size as small as 20 nm.

K. Park J.-S. Kim
Research Center for Biomolecular Nanotechnology,
Department of Environmental Science and Engineering,
Gwangju Institute of Science and Technology (GIST),
261 Cheomdan-gwagiro (Oryong-dong), Buk-gu,
Gwangju 500-712, Republic of Korea
e-mail: kpark@gist.ac.kr

A. L. Miller
National Institute for Occupational Safety and Health/
Spokane Research Lab, Spokane, WA 99207, USA

Introduction

Fine and ultrafine particles in the ambient atmosphere are of current interest due to their effects on the

radiation budget (Intergovernmental Panel on Climate Change 2007), climate change, visibility, and human health. Especially, ultrafine particles and nanoparticles may have higher reactivity and toxicity due to their enhanced surface area-to-volume ratio (Peters et al. 1997; Oberdörster 2000). Those particles in the ambient atmosphere are emitted directly from various sources or formed by gas-to-particle conversion process. The new particles formed can grow to sizes that are optically important and have a potential to affect climate change. Due to their small size and mass, the newly formed particles are easily lost by diffusion and it is difficult to determine their chemical composition. Thus, rapid measurements of physical and chemical properties of nanoparticles are essential to better understand their sources, particle formation and growth mechanisms, and their effects on atmospheric processes and human health.

The development of the aerosol mass spectrometry technique made it possible to directly determine chemical composition of submicron particles in real time, but the detectable size is limited to 50–200 nm depending on the type of aerosol mass spectrometry (Suess and Prather 1999; Noble and Prather 2000; Nash et al. 2006). Recently, by measuring the hygroscopicity of nanoparticles, the composition of the newly formed particles was estimated (Sakurai et al. 2003; Sakurai et al. 2005). This can be done by comparing hygroscopic properties of the freshly formed nanoparticles in the ambient atmosphere with those of standard particles of known hygroscopicity. Hygroscopic properties are key properties of aerosol particles, affecting particle growth by water vapor, scattering efficiency of particles, and potential for the formation of cloud condensation nuclei. Also, an accurate measurement of hygroscopic properties of nanoparticles is essential for better understanding of atmospheric nanoparticle formation and growth. However, there has been limited information on how the hygroscopic properties of atmospheric particles will vary with decreasing size below 50 nm. Hygroscopic properties (deliquescence relative humidity (DRH) and growth factor (GF)) of nanoparticles may or may not be the same as those of submicron or larger particles. For example, theoretical prediction of the GF using the Kelvin correction would not suffice to accurately determine hygroscopic behaviors for such small particles (Hämeri et al. 2000; Hämeri et al. 2001; Russell and Ming 2002).

Thus, this study focuses on how hygroscopic properties (DRH and GF) of nanoparticles vary with their size and structural properties. We combined a hygroscopicity tandem differential mobility analyzer (HTDMA) technique with transmission electron microscopy to measure the hygroscopic properties of various size-resolved nanoparticles such as NaCl, $(NH_4)_2SO_4$, KCl, NH_4NO_3, $MgCl_2$, and $CaCl_2$, which might be possible candidates for constituents of hygroscopic nanoparticles in the ambient atmosphere, and to investigate the potential effect of particle structure or morphology on the hygroscopic properties. Two different particle generation methods (atomizer versus furnace reactor) were used in this study. A combination of nano DMAs and regular DMAs was made to measure particle size change in a wide dynamic particle size range in our HTDMA system.

Experimental

The hygroscopicity tandem differential mobility analyzer (HTDMA) mainly consists of two regular Differential Mobility Analyzers (DMA, TSI 3081) (Knutson and Whitby 1975), two nano Differential Mobility Analyzers (nano DMA, TSI 3085) (Chen et al. 1998), an Ultrafine Condensation Particle Counter (UCPC, TSI 3776), and a humidification system, as shown in Fig. 1. The tandem measurement methods used have been described previously (Radar and McMurry 1986; McMurry and Stolzenburg 1989; McMurry et al. 2002; Park et al. 2003). For our research, test aerosols were generated by using an atomizer (TSI 3076) and a furnace reactor. Particles were first dried to about $\sim$7% RH using a Nafion drier or a diffusion drier, and passed through a ^{210}Po "neutralizer" and then selected according to mobility size with the first nano or regular DMA. The accuracy of all DMAs was tested using the standard PSL particles. The selected particles of a certain size (3–200 nm) were then sent into a humidifier (7–90% RH) and subsequently routed to the second nano or regular DMA and UCPC system to determine particle size change under the elevated relative humidity. The particle size change as a function of RH was used to determine the DRH (i.e., relative humidity at which sudden condensation-driven growth occurs), if exist, and growth factor (the ratio of particle mobility

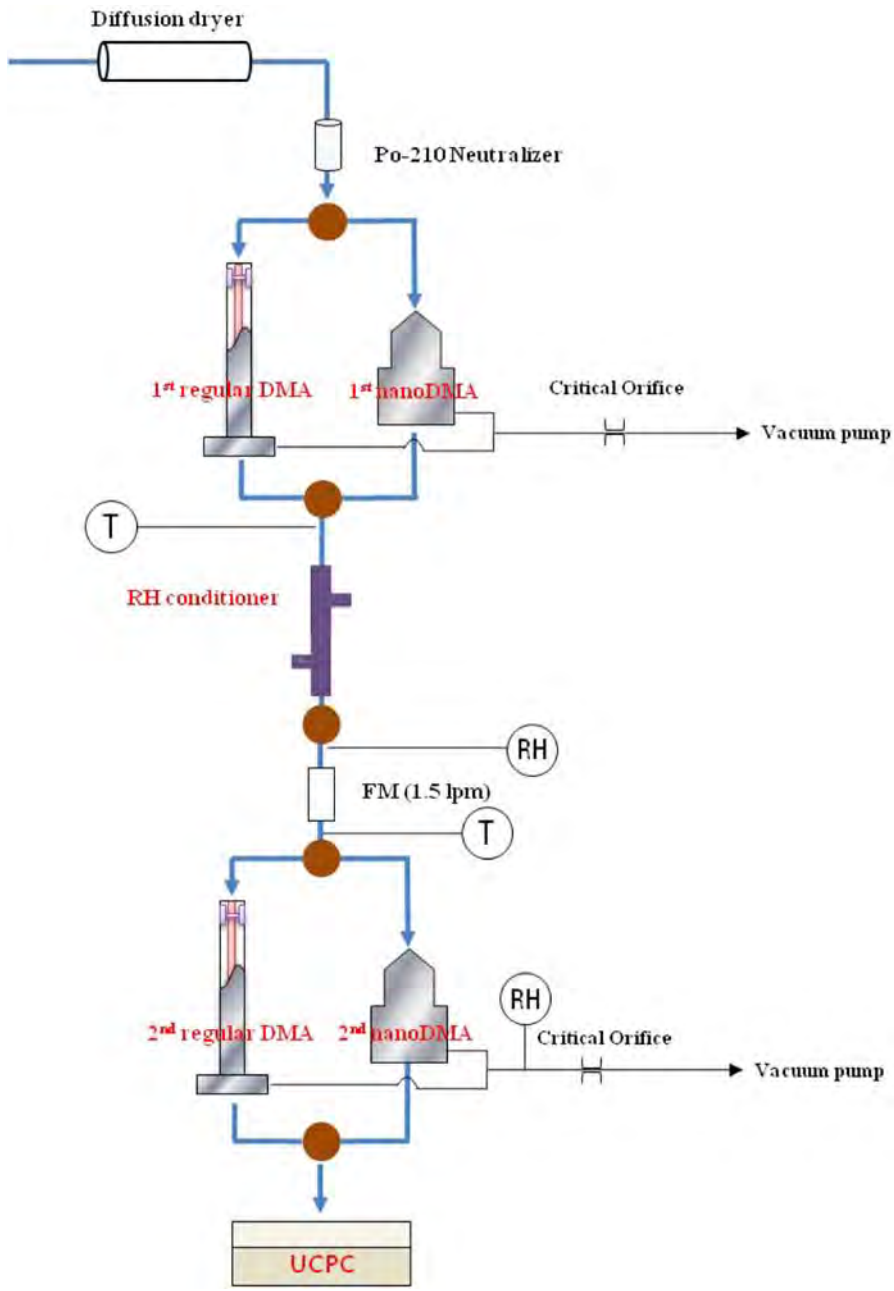

Fig. 1 A schematic of the hygroscopicity tandem differential mobility analyzer (HTDMA) system

diameter at increased RH to that at dry condition). When particles grew to a larger size than the upper size limit ($\sim$80 nm) of the nano-DMA, the second regular DMA was used to measure particle growth. In this way, we are able to determine size-resolved hygroscopic growth of nanoparticles in a wide size range. Relative humidity was measured by capacitance sensors (Omega HX94AV and GE sensing MMR31) with an accuracy of $\pm$2.5% and $\pm$2% RH.

Six types of nanoparticles were chosen for this study (i.e., NaCl, $(NH_4)_2SO_4$, KCl, NH_4NO_3, $MgCl_2$, and $CaCl_2$ particles). These were chosen because they might be considered as possible candidate species for hygroscopic ultrafine particles and nanoparticles in the ambient atmosphere. Particles larger than 30 nm were produced from 0.1% (wt) DI water solution using an atomizer (TSI 3076). To produce particles smaller than $\sim$30 nm, a furnace reactor system

employing an evaporation-condensation method was used. In this method, a quartz boat was placed in the center of the furnace reactor containing 300 mg of sample material and the filtered air was used as a carrier gas. The furnace temperature is set below the melting temperature of the sample (e.g., 200 °C for $(NH_4)_2SO_4$). The material evaporates and subsequently cools quickly upon exiting the furnace causing homogeneous nucleation of nanoparticles. To obtain size distribution of laboratory-generated particles, we used the scanning mobility particle sizer (SMPS) (DMA: TSI 3081, CPC: TSI 3022A). Morphology of the nanoparticles was examined by using a transmission electron microscope (JEOL JEM-2100).

Results and discussion

Table 1 summarizes material properties (density, solubility, surface tension, melting point, boiling point, and theoretical DRH) of the six types of particles tested in this study. During tests, we determined the actual DRH of those nanoparticles by measuring particle GF as a function of relative humidity with the HTDMA technique. Figure 2 shows the GF of NaCl nanoparticles as a function of RH. The NaCl nanoparticles were produced by both an atomizer and a furnace reactor described in the experimental section. The theoretically predicted GF for 8 and 100 nm particles with the Kelvin correction based on calculation by Hämeri et al. (2001) was also included in Fig. 2. As shown, the size of the 100 nm mobility diameter NaCl particles increases abruptly from 100 to 182 nm yielding a GF of 1.82 at ~76% RH, which is close to the theoretical DRH value (75.3% RH) (see Table 1). The 30, 50, and 80 nm NaCl particles were determined to have the same deliquescence behavior as that of the 100 nm particles. However, for particles smaller than 20 nm, we found that the DRH of NaCl particles increased and reached up to ~83% RH for 8 nm NaCl particles. This confirms the conclusions of Biskos et al. (2006a, b), who reported that due to lower surface free energy of the crystalline particles than aqueous particles, the crystalline state is favored, leading to the increase of the DRH. This condition can be described as when the surface tension ratio of the crystalline particles to the aqueous particles is smaller than the diameter ratio of the crystalline particles to the aqueous particles (Biskos et al. 2006a). This suggests that surface property plays an important role in the determination of the DRH and is more pronounced at smaller diameters.

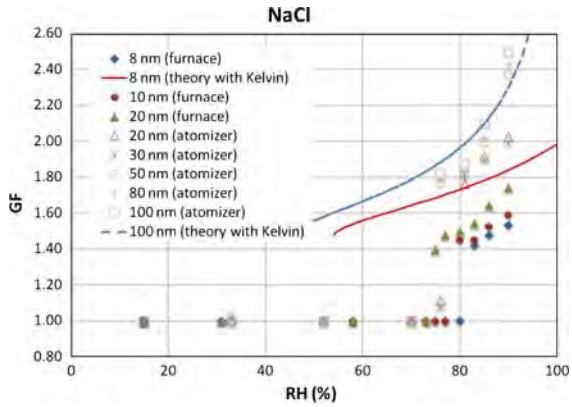

Fig. 2 GF of NaCl nanoparticles as a function of RH including theoretically predicted GF with Kelvin correction (based on calculation by Hämeri et al. 2001)

Table 1 Material properties of particles tested in this study

Name	Formula weight[a] (g/mol)	Density[a] (g/cm^3)	Solubility[a] (g/100 g H_2O)	Surface tension (N/m) at 90% RH	Melting point[a] (°C)	Boiling point[a] (°C)	DRH[a,b] (%)
NH_4NO_3	80.04	1.72	213		170	210	61.8
$(NH_4)_2SO_4$	132.14	1.77	76	0.082	235–280	N/A	79.9 ± 0.5
$CaCl_2$	110.99	2.15	81		772	>1,600	29.0
$MgCl_2$	95.23	2.32	56		712	1,412	33.0
KCl	74.56	1.99	36		790	1,500	84.2 ± 0.3
NaCl	58.45	2.17	36	0.077	800	1,413	75.3 ± 0.1

[a] CRC Handbook (2003)

[b] Seinfeld and Pandis (1998)

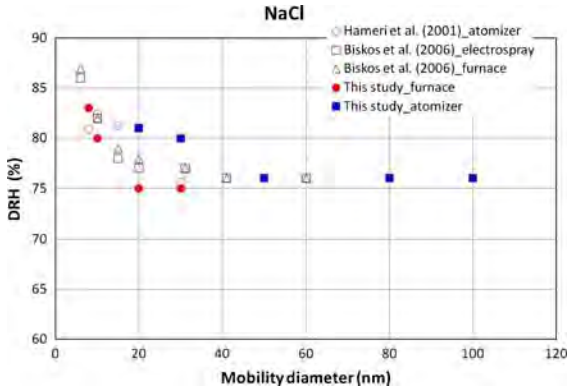

Fig. 3 Size-dependent DRH of NaCl nanoparticles as a function of particle mobility diameter including previous NaCl data (Hämeri et al. 2001; Biskos et al. 2006a)

For the case of 20 nm NaCl nanoparticles, we observed that the DRH of the atomizer-generated particles increased to ~81%, while the DRH of the furnace-generated particles had no increase (i.e., DRH = ~75%). This is not surprising since the surface properties of the furnace-generated NaCl nanoparticles would differ from that of the atomizer-generated NaCl nanoparticles. Our results suggest that the surface tension ratio of the crystalline particles to the aqueous particles would be smaller for the atomizer-generated NaCl particles than the furnace-generated NaCl particles. In other words, the surface free energy of the atomizer-generated NaCl particles is smaller than the furnace-generated NaCl particles. Relatively higher porosity of the furnace-generated NaCl particles may lead to the higher surface free energy, as will be shown in TEM images later in this section. Regardless of the generation method, we did not observe any particle shrinkage or growth with increasing RH at moderate RH below the DRH, suggesting that the NaCl particles did not experience any significant restructuring or water adsorption below the DRH. Figure 3 compares the size-dependent DRH of NaCl nanoparticles as a function of particle mobility diameter with previous data. It shows that the current size-dependent DRH is qualitatively consistent with the previous measurements (Hämeri et al. 2001; Biskos et al. 2006a) and that the amount of increase varies with the generation method for particles smaller than 40 nm.

Figure 4 summarizes average hygroscopic GFs of the sodium chloride nanoparticles at 80% RH, 85% RH, and 90% RH using all measured data. Data clearly showed that growth factor of the sodium chloride nanoparticles decreased as the mobility size decreases. The mobility diameter growth factor at ~80% RH is 1.50 for 10 nm particles compared to 1.89 for 100 nm particles. This can be explained by the enhanced water vapor pressure for nanoparticles due to the Kelvin effect. The theoretical prediction for GF accounting for the Kelvin effect was included in Fig. 4. There is still ~17% difference for 8 nm

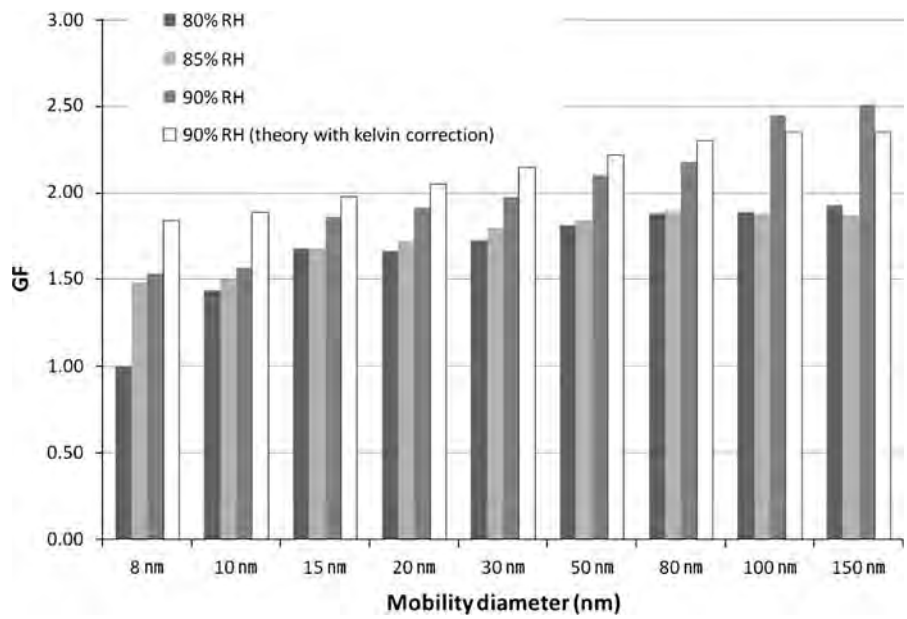

Fig. 4 Hygroscopic growth factors of NaCl nanoparticles averaged at 80% RH, 85% RH, and 90% RH and theoretical values with Kelvin correction at 90% RH (particles smaller than 20 nm was generated by furnace while particles larger than 20 nm were generated by an atomizer)

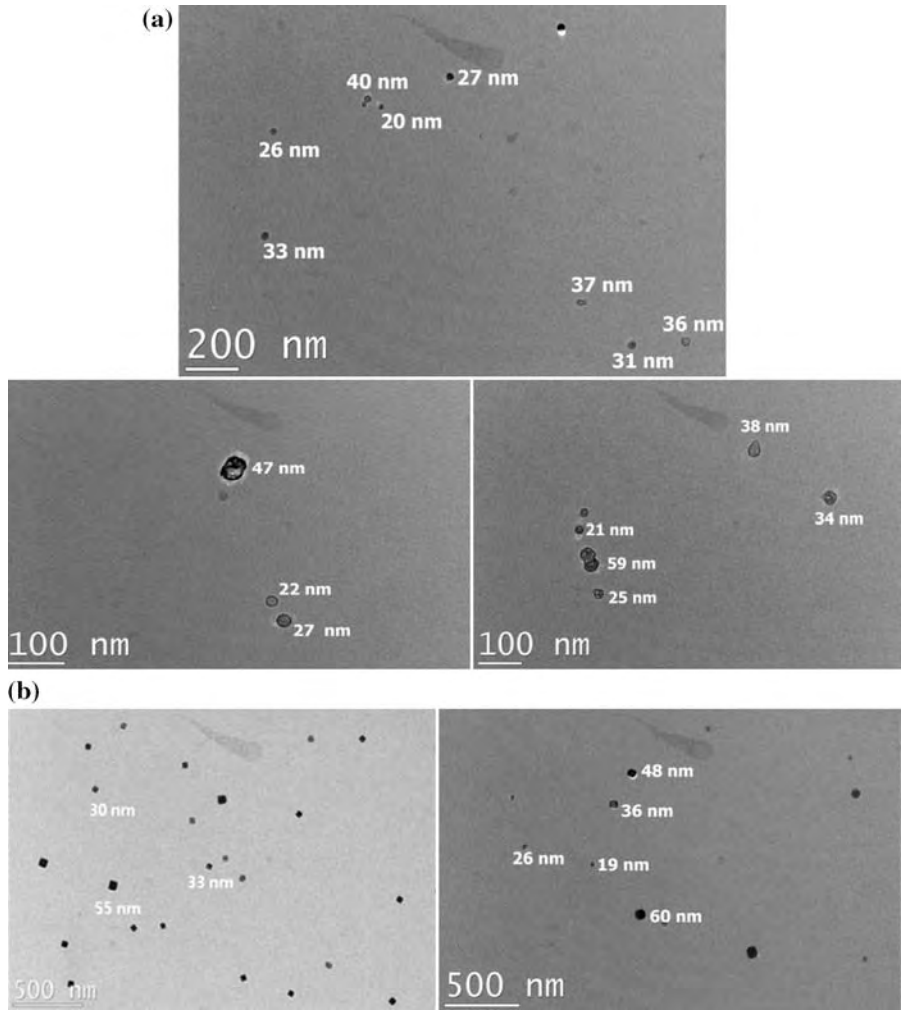

Fig. 5 TEM images for (**a**) furnace-generated NaCl nanoparticles and (**b**) atomizer-generated NaCl particles

particles at 90% RH between the measured GF and the theoretically predicted value with the Kelvin correction. The difference decreased as particle size increased above 50 nm. This suggests that in addition to the Kelvin effect, the size-dependent density and shape of NaCl nanoparticles, which differ from the bulk material density and spherical shape used for calculating the theoretical GF, may play a role in the observed difference. Note that theoretical thermodynamic prediction for the GF is based on the assumption that the particle is perfectly spherical and the solute density is 2.165 g/cm^3 (Lide 2003). Accounting for particle shape using the dynamic shape factor of NaCl, which is known to be 1.08 (Hinds 1999; Biskos et al. 2006b), was not enough to explain the observed difference. We also observed that the GF of the furnace-generated NaCl nanoparticles is smaller than that of atomizer-generated particles having the same size. If the solute density is smaller than the bulk material density, the GF will decrease (Hämeri et al. 2000; Hämeri et al. 2001). It is not certain that the dry salt density of the furnace-generated NaCl nanoparticles is smaller than that of atomizer-generated particles. Voids formed by imperfect crystal growth and trapped water may affect the solute density of the NaCl particles (Weis and Ewing 1999). As shown in Fig. 5a, TEM images for the furnace-generated NaCl nanoparticles showed that they are not perfectly cubic but have somewhat rounded corners and that they have pores and are sometimes aggregates. On the contrary, the atomizer-generated NaCl nanoparticles are perfectly cubic as shown in Fig. 5b. It is possible that the pores and aggregate shape contribute to the smaller density of

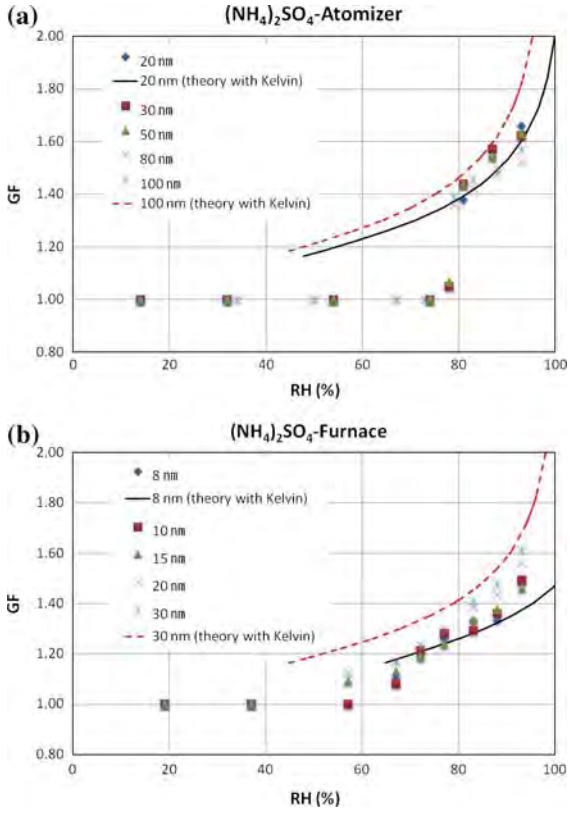

Fig. 6 (**a**) GF as a function of RH for atomizer-generated $(NH_4)_2SO_4$ nanoparticles including theoretically predicted GF based on calculation by Biskos et al. (2006c) and (**b**) GF as a function of RH for furnace-generated $(NH_4)_2SO_4$ nanoparticles including theoretically predicted GF based on calculation by Biskos et al. (2006c)

the furnace-generated NaCl nanoparticles, leading to the smaller GF of the furnace-generated NaCl nanoparticles than that of atomizer-generated particles. Also, particles with pores or voids can trap water leading to lower density.

Figure 6a shows the measured GF as a function of RH for atomizer-generated $(NH_4)_2SO_4$ nanoparticles and included the theoretically predicted GF based on calculation by Biskos et al. (2006c). The DRH of $(NH_4)_2SO_4$ nanoparticles is around 79%, which agrees well with the theoretical value (79.9% RH) (i.e., there is no size-effect on the DRH of $(NH_4)_2SO_4$ nanoparticles contrary to NaCl nanoparticles). Also, the measured GFs agreed with the predicted values for atomizer-generated $(NH_4)_2SO_4$ nanoparticles within 10%. This suggests that the solute density and structure of $(NH_4)_2SO_4$ nanoparticles are not much dependent on size compared to NaCl

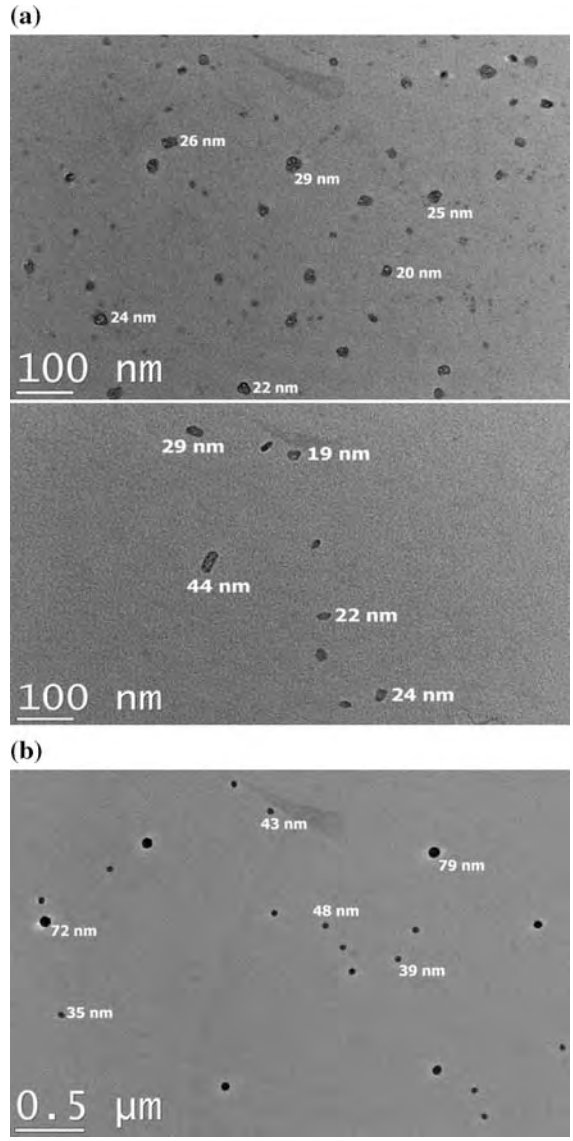

Fig. 7 TEM images for (**a**) furnace-generated $(NH_4)_2SO_4$ particles and (**b**) atomizer-generated $(NH_4)_2SO_4$ particles

nanoparticles. Figure 6b shows the GF as a function of RH for furnace-generated $(NH_4)_2SO_4$ nanoparticles in the size range of 8–30 nm. These $(NH_4)_2SO_4$ nanoparticles showed no significant deliquescence behavior. There is a gradual growth starting at 50–60% RH below the theoretical DRH value of $(NH_4)_2SO_4$ particles (Tang 1980; Tang and Munkelwitz 1993). Water adsorption on to surface of $(NH_4)_2SO_4$ particles at moderate RH can lead to the gradual growth without deliquescence behavior. This occurred only for furnace-generated $(NH_4)_2SO_4$

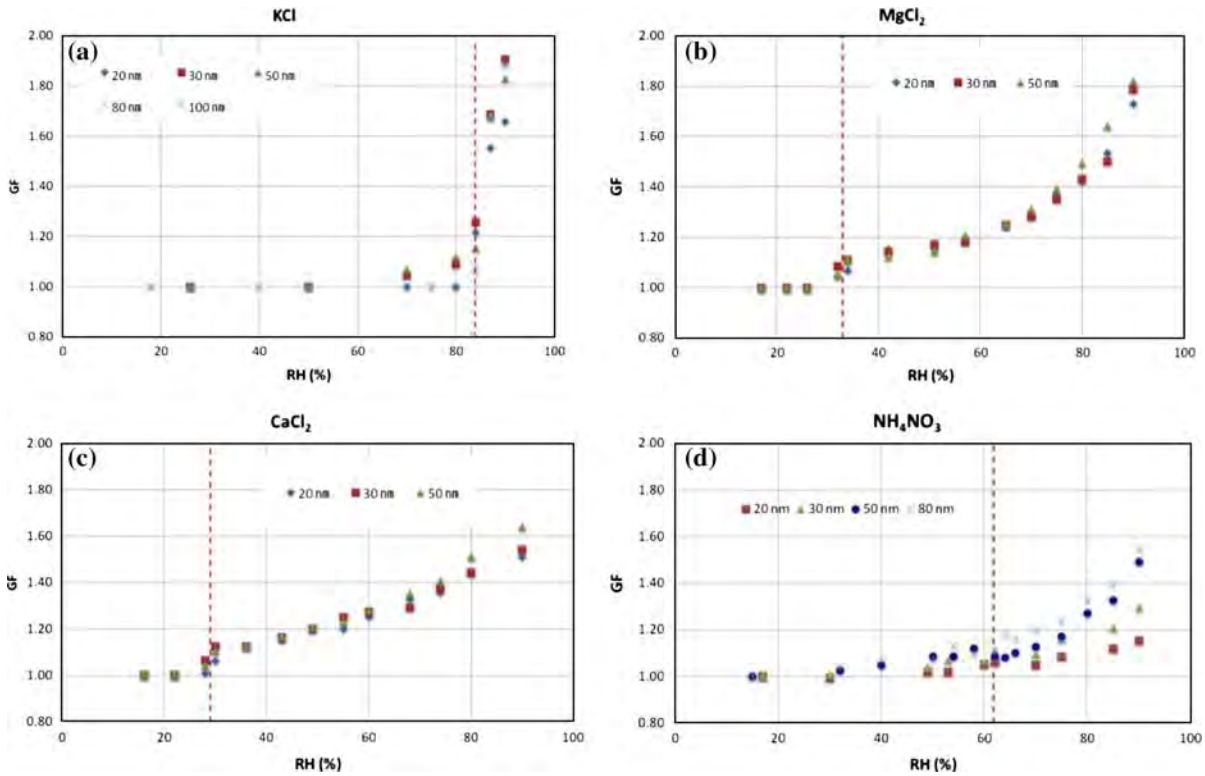

Fig. 8 Hygroscopic GF for (**a**) KCl, (**b**) $MgCl_2$, (**c**) $CaCl_2$, and (**d**) NH_4NO_3 nanoparticles generated by an atomizer (the dotted line represents the DRH of bulk materials)

nanoparticles, which suggests that possibly these nanoparticles may trap water (i.e., not dried out perfectly), causing water adsorption at moderate RH. As shown in Fig. 7, TEM images showed that contrary to atomizer-generated $(NH_4)_2SO_4$ nanoparticles, the furnace-generated particles are not perfectly spherical and are sometime aggregates having pores and holes, which may favor holding residual water even in dried condition. Thus, we argue that hygroscopic growth of the freshly formed ammonium sulfate nanoparticles in the ambient atmosphere may depend on not only composition but also their structure/shape properties.

Figure 8 shows the hygroscopic GFs for KCl, $MgCl_2$, $CaCl_2$, and NH_4NO_3 nanoparticles. The dotted line represents the DRH of bulk materials as included in Table 1. For KCl, $MgCl_2$, and $CaCl_2$ nanoparticles, we observe no significant size-effects on their DRH and GF, while for NH_4NO_3 nanoparticles we observe a size-dependent GF (smaller GF for smaller particles) in the size range of 20–100 nm. Also, NH_4NO_3 nanoparticles have no abrupt deliquescence behavior and a gradual growth below the theoretical DRH (61.8% RH). More research is required to determine what makes different deliquescence behaviors for NH_4NO_3 nanoparticles.

Conclusion

By using a HTDMA technique, we examined size-effect of six-types of nanoparticles (NaCl, $(NH_4)_2SO_4$, KCl, NH_4NO_3, $MgCl_2$, $CaCl_2$) on their hygroscopic properties. Our data suggest that structure properties of NaCl and $(NH_4)_2SO_4$ nanoparticles affect the DRH and GF. NaCl nanoparticles were shown to have an increased DRH (83% RH at 8 nm) and their GFs below $\sim$50 nm were smaller than theoretically predicted values using the Kelvin correction. The GF of the furnace-generated NaCl nanoparticles that have pores and aggregate shape was found to be smaller than that of atomizer-generated particles that are perfectly cubic. For the case of atomizer-generated $(NH_4)_2SO_4$ nanoparticles, the measured DRH and GF values

agreed well with those found in the literature value. However, for furnace-generated $(NH_4)_2SO_4$ nanoparticles, we observed a gradual growth at moderate RH without deliquescence behavior. TEM images indicated that the furnace-generated $(NH_4)_2SO_4$ nanoparticles are not perfect spheres and are sometime aggregates having pores and holes, which may favor holding residual water even in the dried condition. No significant size-dependent hygroscopic behaviors occurred for KCl, $MgCl_2$, and $CaCl_2$ nanoparticles for the mobility size as small as 20 nm. Our results suggest that when hygroscopic data of atmospheric nanoparticles are investigated, the specific size-dependent hygroscopic behaviors for different types of nanoparticles must be accounted for and that structural properties of nanoparticles should be determined for certain types of nanoparticles.

Acknowledgments The research described in this article was supported by Eco Science-Technology Advancement Research Project. It was partially supported by Korea Research Foundation Grant (KRF-2007-331-D00222) and Korea Science and Engineering Foundation (KOSEF) (No. R01-2007-000-10391-0).

References

Biskos G, Malinowski A, Russell LM, Buseck PR, Martin ST (2006a) Nanosize effect on the deliquescence and the efflorescence of sodium chloride particles. Aerosol Sci Technol 40:97–106. doi:10.1080/02786820500484396

Biskos G, Russell LM, Buseck PR, Martin ST (2006b) Nanosize effect on the hygroscopic growth factor of aerosol particles. Geophys Res Lett 33:L07801

Biskos G, Paulsen D, Russell LM et al (2006c) Prompt deliquescence and efflorescence of aerosol nanoparticles. Atmos Chem Phys 6:4633–4642

Chen D-R, Pui DYH, Hummes D, Fissan H, Quant FR, Sem GJ (1998) Design and evaluation of a nanometer aerosol differential mobility analyzer (Nano-DMA). J Aerosol Sci 29(5):497–509. doi:10.1016/S0021-8502(97)10018-0

Hämeri K, Vakeva M, Hansson HC, Laaksonen A (2000) Hygroscopic growth of ultrafine ammonium sulphate aerosol measured using an ultrafine tandem differential mobility analyzer. J Geophys Res 105:22231–22242. doi:10.1029/2000JD900220

Hämeri K, Laaksonen A, Vakeva M, Suni T (2001) Hygroscopic growth of ultrafine sodium chloride particles. J Geophys Res-Atmos 106:20749–20757. doi:10.1029/2000JD000200

Hinds WC (1999) Aerosol technology. Wiley-Interscience, New York

Intergovernmental Panel on Climate Change (2007) Climate change 2007. Cambridge University Press, New York

Knutson EO, Whitby KT (1975) Aerosol classification by electric mobility: apparatus, theory, and applications. J Aerosol Sci 6:443–451. doi:10.1016/0021-8502(75)90060-9

Lide DR (2003) CRC handbook of chemistry and physics, 84th edn. CRC Press, London

McMurry PH, Stolzenburg MR (1989) On the sensitivity of particle size to relative humidity for Los Angeles aerosols. Atmos Environ 23:497–507. doi:10.1016/0004-6981(89)90593-3

McMurry PH, Wang X, Park K, Ehara K (2002) The relationship between mass and mobility for atmospheric particles: a new technique for measuring particle density. Aerosol Sci Technol 36:227–238. doi:10.1080/02786822753504083

Nash DG, Baer T, Johnston MV (2006) Aerosol mass spectrometry: an introductory review. Int J Mass Spectrom 258:2–12. doi:10.1016/j.ijms.2006.09.017

Noble CA, Prather KA (2000) Real-time single particle mass spectrometry: a historical review of a quarter century of the chemical analysis of aerosols. Mass Spectrom Rev 198:248–274. doi:10.1002/1098-2787(200007)19:4<248::AID-MAS3>3.0.CO;2-I

Oberdörster G (2000) Toxicology of ultrafine particles: in vivo studies. Philos Trans Math Phys Eng Sci 358:2719–2739

Park K, Cao F, Kittelson DB, McMurry PH (2003) Relationship between particle mass and mobility for diesel exhaust particles. Environ Sci Technol 37:577–583. doi:10.1021/es025960v

Peters A, Wichmann HE, Tuch R, Heinrich J, Heyder J (1997) Respiratory effects are associated with the number of ultrafine particles. Am J Respir Crit Care Med 155:1367–1383

Radar DJ, McMurry PH (1986) Application of the tandem differential mobility analyzer to studies of droplet growth or evaporation. J Aerosol Sci 17:771–787. doi:10.1016/0021-8502(86)90031-5

Russell LM, Ming Y (2002) Deliquescence of small particles. J Chem Phys 116:311–321. doi:10.1063/1.1420727

Sakurai H, Tobias HJ, Park K, Zarling D, Docherty S, Kittelson DB et al (2003) On-line measurements of diesel nanoparticle composition and volatility. Atmos Environ 37:1199–1210. doi:10.1016/S1352-2310(02)01017-8

Sakurai H, Fink MA, McMurry PH, Mauldin L, Moore KF, Smith JN et al (2005) Hygroscopicity and volatility of 4–10 nm particles during summertime atmospheric nucleation events in urban Atlanta. J Geophys Res 110:D22S04. doi:10.1029/2005JD005918

Seinfeld JH, Pandis SN (1998) Atmospheric chemistry and physics. Wiley-Interscience, New Jersey

Suess DT, Prather KA (1999) Mass spectrometry of aerosols. Chem Rev 99:3007–3025. doi:10.1021/cr980138o

Tang IN (1980) On the equilibrium partial pressures of nitric acid and ammonia in the atmosphere. Atmos Environ 14:819–828. doi:10.1016/0004-6981(80)90138-9

Tang IN, Munkelwitz HR (1993) Composition and temperature dependence of the deliquescence properties of hygroscopic aerosols. Atmos Environ 27:467–473

Weis DD, Ewing GE (1999) Water content and morphology of sodium chloride aerosol particles. J Geophys Res-Atmos 104:21275–21285. doi:10.1029/1999JD900286